

Experimental Investigation of Parameters for C45(AISI-1045) to Enhance the Welding Strength

¹C. Labesh Kumar

Associate Professor, Department of Mechanical Engineering
Institute of Aeronautical Engineering, Dundigal, Hyderabad

²M. Yeswanth Reddy; ³K. Murali Mohan
Students of Mechanical Engineering, IARE

Abstract:- An experimental investigation was conducted to identify and optimize the factors influencing the welding strength of C45 (AISI-1045) steel. C45, a medium carbon steel known for its excellent machinability and high strength, is frequently employed in applications requiring significant tensile strength and hardness. The 10 mm thick medium carbon steel plate was welded using Metal Inert Gas Welding. For Gas Metal Arc Welding (GMAW), the deposited thickness is 10 mm, with a qualified range of 3 to 20 mm (multi-run). This study offers a thorough evaluation of various research efforts in the realm of GMAW of steel, aiming to illustrate the impact of process variables and input parameters on weld quality characteristics. To achieve this, detailed literature reviews and comparisons of diverse findings were performed, and insights were synthesized. Where discrepancies in parameter effects were identified, appropriate explanations and justifications were provided. Consequently, it was determined that arc voltage, welding current, wire feed rate, and travel speed have a substantial impact on weld quality (particularly regarding penetration, bead height, bead width, and heat-affected zone) in comparison to other parameters examined. This indicates that accurately establishing the optimal combination of welding parameters especially arc voltage, welding current, wire feed rate, and travel speed—results in the desired quality level of the weldment.

Keywords:- Metal Inert Gas Welding, Welding Parameters, Weld Quality Characteristics, Steel Materials, Process Condition.

I. INTRODUCTION

Welding is one of the most cost-effective and efficient methods for creating permanent joints. It is a common process across various industries. Different types of welding are employed in industries based on their specific applications, such as Tungsten Inert Gas (TIG), Shielded Metal Arc Welding (SMAW), Gas Tungsten Arc Welding (GTAW), Electron Beam Welding (EBW), Laser Beam Welding (LBW), and Friction Stir Welding (FSW). For this work, Gas Metal Arc Welding (GMAW) was utilized. C45 refers to a steel grade that has a medium amount of carbon in its makeup, with its technical designation being AISI 1045, which is equivalent to EN-8. It is available in several forms, including rolled, forged, normalized, bright drawn, or smooth turned,

and it provides excellent strength, toughness, and resistance to wear. This steel is used in the production of components such as sprockets, axle bolts, connecting rods, studs, rams, pins, crankshafts, torsion bars, worm guide rods, and roll spindles. C45 contains approximately 0.45% carbon and also has small quantities of silicon (Si), phosphorus (P), and sulphur (S), along with manganese (Mn). The chemical makeup of C45 steel is detailed below:

C, Mn, Si, P, S, Cr, and M

The test sample is subjected to a spark emission spectroscopy examination (ASTM-E 415:2015 Standard), which is utilized for analysing its chemical composition. The primary parameters of Gas Metal Arc Welding (GMAW) with medium carbon steels such as C45 (AISI-1045) include welding current, arc voltage, wire feed rate, travel speed, and the flow rate of shielding gas. This study aims to elucidate the significant characteristics and effects of robotic, automatic, and semi-automatic GMAW input parameters on the quality of welds. Among the various input factors, arc voltage, welding current, wire feed rate, travel speed, contact tip-to-work distance (CTWD), shielding gas flow rate, electrode work angle, and heat input are analysed to understand how each factor influences the weld quality of steel materials. Gas Metal Arc Welding (GMAW), often referred to as MIG (Metal Inert Gas) welding, can accommodate a minimum thickness of approximately 0.6 mm (0.024 in) and a maximum thickness that can reach several centimetres or more. For the GMAW process, we opted for an 80-20 mixture of argon and carbon dioxide for spray transfer applications. Argon offers superior shielding compared to other gases; however, its low thermal conductivity can destabilize material transfer or deposition. On the other hand, CO₂ enhances the deposition rate and penetration. Therefore, we chose to use a blend of argon and CO₂ gas to balance these properties.

Gas metal arc welding (GMAW) is recognized as the most commonly utilized welding technique due to its benefits, including rapid speed, effective arc performance, and the quality of welded joints. Typically, GMAW is applied to weld SS409L, and the mechanical characteristics of these welded joints are influenced by the chemical makeup of the weld metal. This composition is affected by various factors such as bead geometry. Percent dilution, which quantifies the proportion of the melted base metal relative to the overall weld deposit volume, along with weld bead geometry, are

shaped by welding parameters like speed, current, and voltage. Numerous studies have been referenced that outline strategies for optimizing welding process conditions to achieve the desired weld bead shape. These strategies include the Taguchi method for gas tungsten arc welding, mathematical modelling for dip arc welding, regression modelling for laser butt welding, and factorial tests concerning stainless steel coatings. The parameters of the welding process are crucial in determining the percentage of dilution and the geometry of the weld bead (including factors such as bead width, height, and penetration). Both percentage dilution and weld bead geometry are critical in assessing joint quality. The current study aims to examine how varying welding speeds (300, 400, and 500 mm/minute) impact percentage dilution and weld bead shape. The GMAW of ferritic stainless steel SS409L with austenitic stainless steel filler wire ER304L using pure argon gas has been conducted. An analysis of percentage dilution and weld bead geometry has been performed. It has been observed that as welding speed increases, bead width, height, and penetration diminish, while the percentage of dilution first rises with welding speed and then falls upon further increases of these parameters [1].

The characteristics of weldment quality are primarily indicated by the heat-affected zone (HAZ), the geometry of the weld bead, depth of penetration, microstructure, and mechanical properties. Accordingly, the quality assessment of a weld joint can be influenced by various factors such as surface and internal imperfections. Surface flaws consist of issues like lack of fusion, incomplete penetration, excessive convexity, overly deep penetration, significant asymmetry, excessive throat thickness, inadequate throat thickness, and spatter. Similarly, internal flaws encompass cracks, porosity, inclusions, lack of fusion, and inadequate penetration. The wire feed rate significantly impacts the depth of penetration.

The deposition rate is primarily influenced by various parameters, with the wire feed rate being the most significant factor. By increasing the wire feed rate, more molten metal is deposited, which enhances the depth of penetration. A higher feed rate contributes to an increased amount of heat introduced into the weld pool area, leading to greater penetration depth. The wire feed rate is a crucial input variable that impacts bead height as well. This parameter significantly influences the weld area calculation, explaining 33.48% of the variation within a linear model. Although welding wire serves as filler metal, a higher wire feed rate is positively associated with bead height, resulting in a greater quantity of filler material deposited each second. An increase in the wire feed rate also translates to a wider bead due to the higher volume of material being deposited within the weld joint. Elevating the wire feed rate raises the joining temperature, and the melting of a substantial amount of filler wire into the weld pool contributes to an increase in bead width. Suitable electrodes for gas metal arc welding (GMAW) of C45 (AISI 1045) steel include E7018, E9018, and ER70S-6. It is advisable to select an electrode with low hydrogen content and low alloy when working with C45. A total of 27 experiments were conducted in this study. The AHP-MOORA and ASRS methods were applied to optimize the MIG welding process parameters, and the results

indicated improved penetration in the weld achieved through the use of fluxes like SiO₂ and Cr₂O₃. Based on the current findings, it is suggested that centripetal Marangoni convection and a constricted arc mechanism contribute to increasing the penetration in activated MIG welding. The hardness of the welded joint was assessed using Vickers hardness testing [2]. The goal is to compare different welding methods, including gas metal arc welding (GMAW), gas tungsten arc welding (GTAW), shielded metal arc welding (SMAW), and submerged arc welding (SAW), to evaluate their effect on the strength of welds. Factors such as welding current, voltage, travel speed, heat input, shielding gas composition, and preheating temperature can have a major impact on weld strength. These parameters can be adjusted either separately or in conjunction to analyze their effects. The joint design, encompassing geometry, fit-up, and preparation techniques like bevelling or chamfering, plays a role in determining weld strength. Various joint configurations may be tested to explore their influence on welding strength. Differences in the medium carbon steel's composition, including alloying elements or impurities, could affect the strength of the weld. Experiments may compare different grades or types of steel. Post-weld heat treatment techniques, such as annealing, quenching, or tempering, can alter the microstructure and mechanical characteristics of the weld. Different heat treatment conditions may be applied to investigate their impact on welding strength. Various mechanical testing approaches, such as tensile testing, bend testing, impact testing, or hardness testing, can be used to assess the strength of the welded joints. The selected testing method can affect the observed welding strength.

II. METHODOLOGY

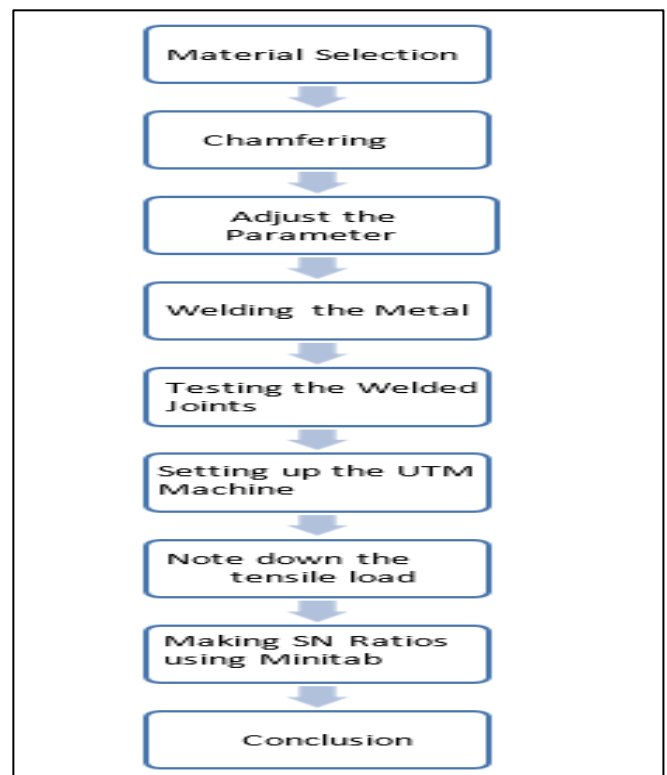


Chart 1 Flow Chart of Welding Process and Testing the Joints

III. PROJECT IMPLEMENTATION

The sample is fabricated according to the ASME welding standards. Using a band saw, the strip is roughly cut into two halves measuring 100*50*10 (mm) each. A chamfer is applied to each sample using a milling machine, creating a single V groove with a combined angle of 45°.

➤ *The Chemical Composition for the C45 Steel:*

Table 1 The Chemical Composition for the C45 Steel

Carbon	Manganese	Silicon	Sulphur	Phosphorus
0.45%	0.76%	0.23%	0.026%	0.034%

- **Shielding Gas:** 80% Argon (Ar) / 20% CO2 at 20 lpm.
- **Filler Material:** ER70S-6 wire with a diameter of 1.0 mm.

The blade of the saw risks wearing down as C45 welding becomes harder. Gas and laser cutting methods are ineffective for this material because the heat can influence the weld's integrity, leading to undesirable changes in microstructure in both the weld zone and the heat-affected zone. To address these limitations, water jet cutting was selected for the following reasons:

- It is capable of cutting nearly all hard materials.
- Water jets can handle material thicknesses of up to 500 mm.
- It offers a cutting tolerance of ± 0.45 mm.
- It operates as a cold-cutting method, remaining unaffected by heat.



Fig 1 C45 Plate

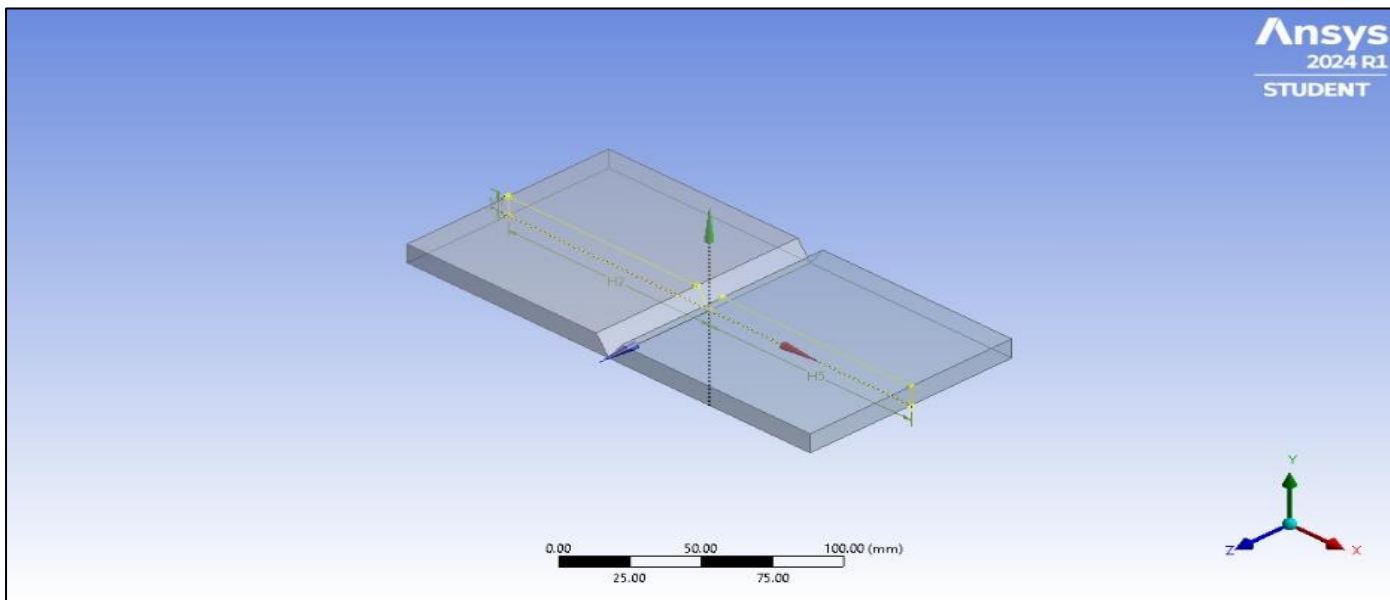


Fig 2 Ansys Design

For GMAW, we selected an 80-20 mixture of Argon and carbon dioxide for spray transfer. Argon offers superior shielding compared to other gases. However, the drawback of argon is its low thermal conductivity, which affects the stability of material transfer or deposition. CO2 gas enhances deposition rate and penetration. Therefore, to balance this, we opted for the Ar-CO2 gas mixture. We have established several parameters for the welding process, including arc

voltage, welding current, wire feed rate, shielding gas flow, and root gap. For our experimentation we are taking three parameters as consideration, they are:

- Arc voltage (V)
- Welding current(A)
- Root gap(mm)

• *Mechanical Properties of C45:*

Table 2 Mechanical Properties of C45

S. No	Mechanical Properties	Range
1	Tensile strength	570–700 MPa
2	Yield strength	230–275 MPa
3	Hardness	170–210 Brinell
4	Density	7.87 g/cm ³
5	Melting temperature	1495°C

• *Machine Specifications of MIG Welding:*

Table 3 Machine Specifications of MIG Welding

S. No	Specifications	Range
1	Arc voltage	84V-96V
2	Welding current	20A-40A

By meticulously managing these parameters and carrying out a comprehensive experimental study, it is feasible to obtain high-quality welds in C45 steel. This will guarantee the structural integrity and longevity of welded components, leading to enhanced performance and dependability. MIG welding, or Gas Metal Arc Welding (GMAW), is a highly adaptable and effective method for joining metals that is extensively used across various industries. This technique utilizes a continuously supplied

wire electrode that serves as both the filler material and the conduit for electrical current. MIG welding is particularly valued for its capability to work with a range of materials, such as mild steel, stainless steel, and medium-carbon steel like C45 steel.

• *The Experimentation Table for the Welding Process:*

Table 4 The Experimentation Table for the Welding Process

Experimentation Method	Arc voltage(V)	Welding current(A)	Root gap(mm)
1.	20	110	1
2.	20	115	2
3.	20	120	3
4.	22	110	2
5.	22	115	3
6.	22	120	1
7.	24	110	3
8.	24	115	1
9.	24	120	2



Fig 3 Before Welding

It helps to ensure the molten pool is stable without excessive spatter. With a higher current, you can achieve deeper penetration, which is essential when welding thicker sections. This is particularly useful for V-butt joints with wider root gaps (2mm or 3mm), ensuring good fusion at the root and the sides of the joint. This is a very tight gap,

requiring precise control over the welding technique. At this gap, you need to ensure that the weld bead is focused and the heat input is controlled to avoid burn-through. A lower current and voltage may be required to prevent excessive melting at the root. This is a moderate gap, which is commonly used in most MIG welding applications. It allows

for sufficient penetration while reducing the risk of defects like lack of fusion. The combination of 22V arc voltage and 115A current is ideal for filling a 2mm root gap in C45 steel, providing a strong, clean weld. With a larger gap, you need higher heat input to ensure complete penetration. A 24V arc voltage and 120A current setting would be beneficial for a 3mm root gap, ensuring that the weld metal fills the entire gap and provides a strong bond between the two workpieces.

Start the weld at the base of the V-butt joint. Position the MIG gun at a suitable angle, usually between 10° and 15° relative to the workpiece, making sure that the nozzle points toward the leading edge of the joint as shown in fig4. This

torch angle is crucial for regulating the shape and penetration of the bead. Maintain a stable arc by managing the speed and distance of the torch. An elongated arc may lead to inadequate penetration, while a shorter arc can result in spatter. For the V-butt joint, utilize a weaving technique (moving the MIG gun side to side) to guarantee complete fusion across the joint, particularly if there is a wider root gap. The width of the weave should be modified depending on the size of the joint and root gap. It is important to control the heat input to prevent burn-through or distortion of the workpiece. This can be achieved by regulating the travel speed and ensuring consistent arc voltage and current.



Fig 4 After Welding

Configure the testing parameters, such as load rate, strain rate, and maximum load. Ensure that the UTM is calibrated to yield accurate and dependable results. This entails checking the load cell, displacement transducers, and other pertinent components. Initiate the test by applying a

controlled load or displacement to the specimen. Continuously observe the load and deformation data shown on the UTM's control panel or computer interface. Document the load and deformation data at regular intervals or continuously throughout the duration of the test.

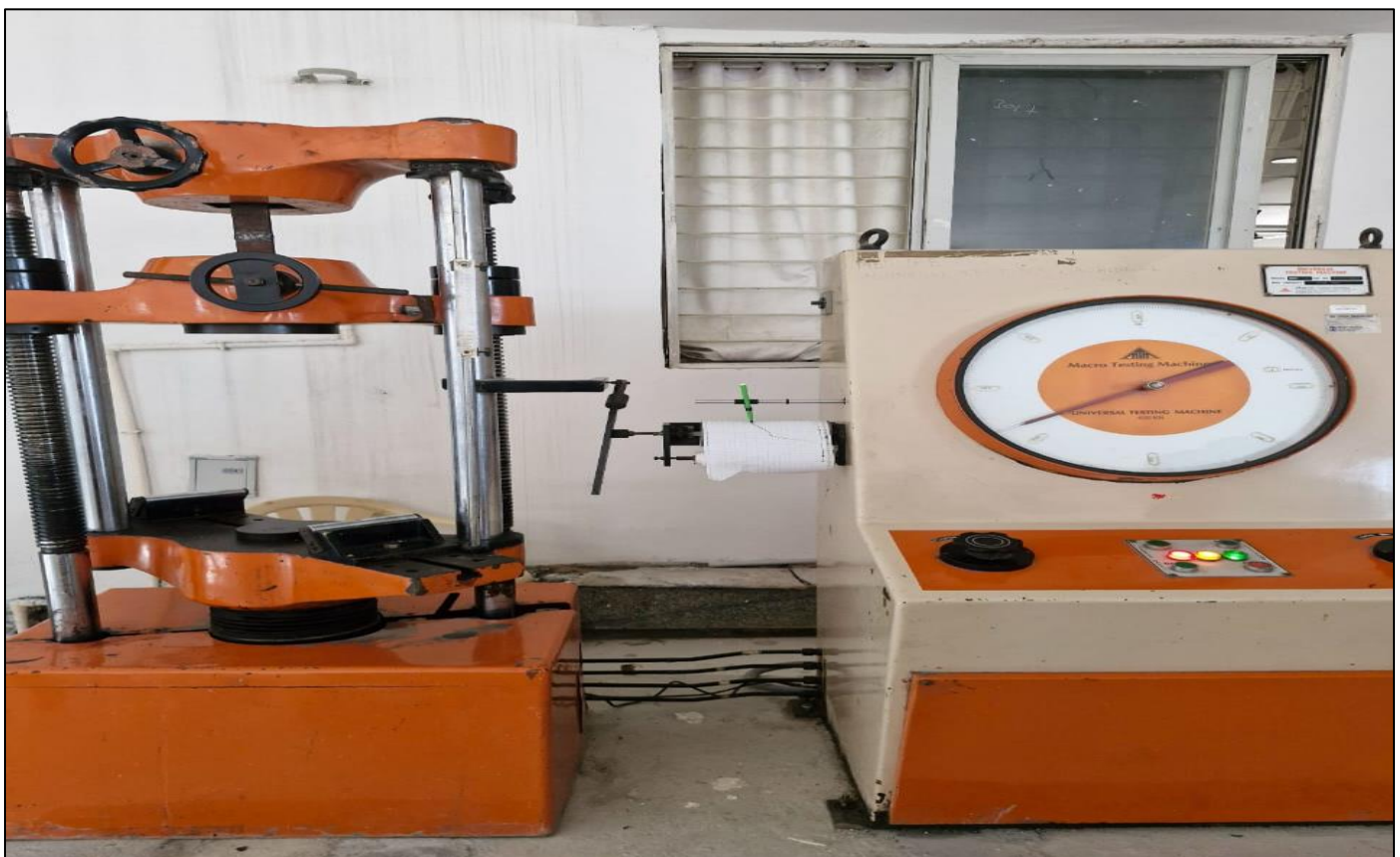


Fig 5 Universal Testing Machine

Once the specimen is correctly positioned, begin the test by launching the software or pressing the “Start” button located on the control panel. The machine will start applying force to the specimen at the predetermined rate. In a tensile test, the crosshead will move upward to exert tension on the specimen. During the test, continually observe the machine’s performance and verify that the load and displacement values remain within the specified limits. Most UTM machines feature real-time data acquisition systems that present force versus displacement graphs, allowing you to monitor the material’s response as it deforms under stress. At some point during the tensile test, the specimen will reach its breaking point and fracture. The UTM will cease operation once the specimen has failed, and it will log the maximum force

applied, elongation, and other essential parameters. After the specimen has failed or the test concludes, halt the machine. Carefully examine the specimen for indications of failure, which may include fracture, rupture, or permanent deformation. Most UTM software will produce a comprehensive test report that includes graphs and calculations of the material properties. This report acts as documentation for the material’s performance under defined conditions and is crucial for quality control, product development, and adherence to material standards. Utilizing a Universal Testing Machine involves a detailed process that requires thorough setup, operation, and analysis. By grasping the components, adhering to the correct procedures, and observing safety measures.



Fig 6 Specimen after Break

IV. RESULT AND DISCUSSION

Table 5 Tensile Load after Testing the Welded Joints

S. No	Arc voltage(V)	Welding current(A)	Root gap(mm)	Tensile load (KN)
1.	20	110	1	328
2.	20	115	2	300
3.	20	120	3	312
4.	22	110	2	305
5.	22	115	3	287
6.	22	120	1	293
7.	24	110	3	292
8.	24	115	1	284
9.	24	120	2	288

➤ Mean Effective Plot Graphs

Mean effective plot graphs serve as essential tools in statistical analysis, providing a visual depiction of average results across various groups or conditions, which aids in recognizing trends, relationships, and data variations. By offering a straightforward representation of the impact that different factors have on a response variable, these plots facilitate more informed decision-making and simpler interpretation of both experimental and observational data. Mean plots, frequently utilized in areas such as quality control, experimental design, and process optimization, allow researchers and practitioners to identify patterns, improve conditions, and highlight areas that may need additional focus.

To generate a mean effective plot graph using Minitab, which is a widely used statistical software, the initial step involves organizing the data. Generally, the data should be arranged with one column for the factor levels (like different treatments, conditions, or time points) and another column for the response variable (such as measurements, performance metrics, or test results). The factor levels denote the independent variables being examined, while the response variable reflects the dependent variable, or the outcome that you are aiming to measure or predict. After entering the data correctly into Minitab, the following step is to create the plot. This is accomplished by going to the "Graphs" menu, where you will find options such as "Mean Plot" or "Interaction Plot." The choice of plot is dependent on the type of analysis you are conducting. A Mean Plot is primarily used when you

want to assess how the response variable behaves across various factor levels, while an Interaction Plot is beneficial for exploring how several factors influence each other and impact the response variable. When selecting the appropriate

variables for the plot, you'll typically define the factor(s) or grouping criteria such as different treatments, time periods, or experimental conditions and then select the corresponding response variable.

Table 6 Response Table for Signal to Noise Ratios

Level	Current	Voltage	Root Gap
1	49.91	49.77	49.57
2	49.39	49.26	49.47
3	49.19	49.47	49.45
Delta	0.73	0.51	0.12
Rank	1	2	3

Table 7 Response Table for Means

Level	Current	Voltage	Root Gap
1	313.3	308.3	301.7
2	295.0	290.3	297.7
3	288.0	297.7	297.0
Delta	25.3	18.0	4.7
Rank	1	2	3

In conclusion, mean effective plot graphs are a powerful visual tool for analyzing data in various domains, from research to manufacturing and quality control. By enabling easy comparison of averages across different factor levels or conditions, these plots facilitate the identification of trends, optimal settings, and areas for improvement. With Minitab's intuitive interface, creating and interpreting mean effective plots is straightforward, making them an essential tool for decision-making, process optimization, and data-driven analysis.

The graph illustrates a significant drop in the average response as the current rises from 110 to 120. At a current of 110, the average response reaches its peak, approximately 315. By the time the current hits 120, the mean response falls to its lowest point, around 290. This pattern in table 4.4 indicates that lower current levels correlate with a more

favorable response, highlighting a strong negative correlation between current and the average response. The impact of voltage on the response exhibits a non-linear pattern. Starting at 20, the average response is relatively high (just over 300), but then it decreases to its lowest point at 22 (roughly 285) before climbing back up at 24 (just under 295). This U-shaped trend implies that voltages of about 20 or 24 may be more advantageous compared to 22. The response gradually declines as the root gap increases from 1 to 3. Although this effect is not as pronounced as that of current or voltage, the trend suggests that a smaller root gap could lead to a somewhat better average response. Current exerts the most considerable influence, with a sharp reduction in response as current values rise. Voltage shows a non-linear impact, indicating that 20 and 24 could be more beneficial. The root gap has a mild and consistent negative effect on the response.

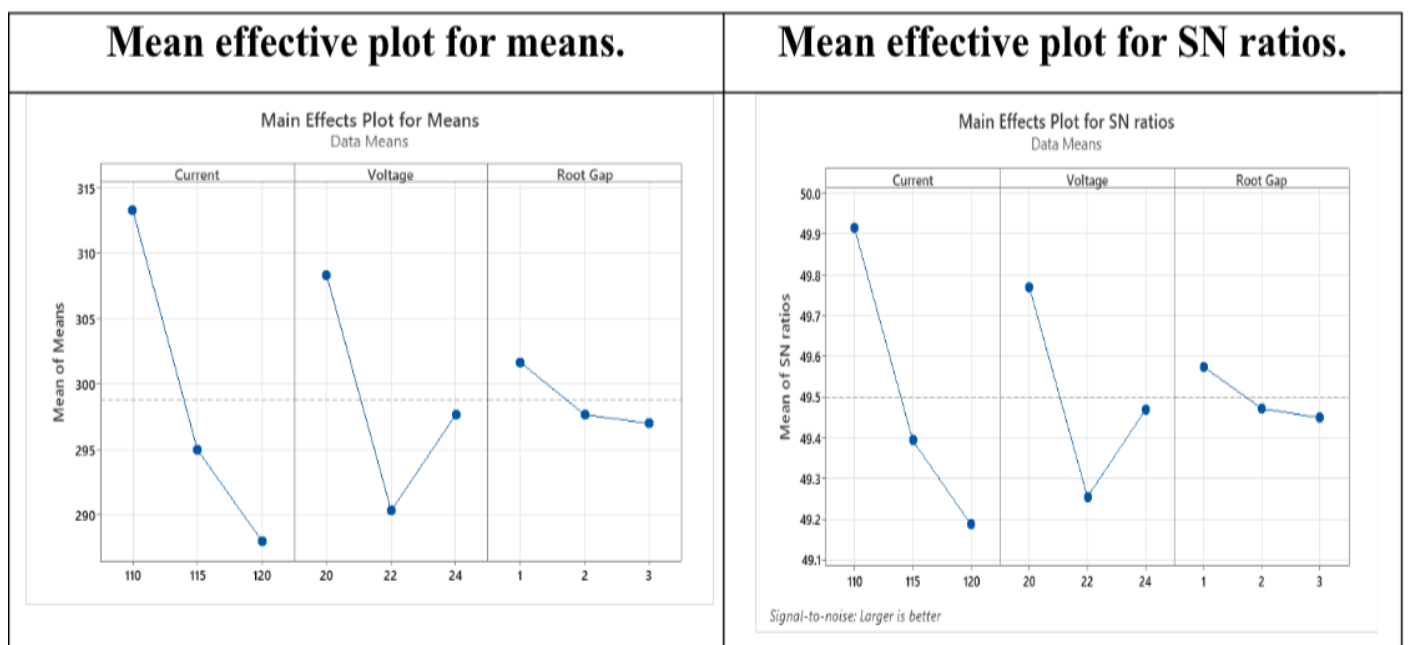


Fig 7 Mean effective plot graphs.

The graph illustrates that as the current rises from 110 to 120, the signal-to-noise (SN) ratio declines. This implies that an increased current level results in a lower quality output. The graph shows that the SN ratio increases as the voltage goes from 20 to 22, before experiencing a slight decrease at 24. This indicates that an intermediate voltage might be ideal for maximizing the SN ratio. The graph depicts a downward trend in the SN ratio as the root gap expands from 1 to 3. This suggests that a smaller root gap could be more advantageous for achieving a higher SN ratio. According to the graph, it seems that the current and root gap have a more pronounced effect on the SN ratio than the voltage. To enhance the process for a better SN ratio, it may be useful to explore lower current levels and a reduced root gap. However, further analysis and possibly more experiments would be necessary to validate these observations and determine the best settings for all three factors. The graph only displays the primary effects of each variable. Nonetheless, there may be interaction effects among the factors, indicating that the influence of one variable could rely on the level of another. To thoroughly comprehend the effects of these variables, it is critical to consider potential interaction effects. Evaluating the statistical significance of the noted trends is also essential. Statistical analyses can aid in assessing whether the differences observed in the SN ratios are statistically meaningful or merely due to random fluctuations. The optimal conditions suggested based on the graph may not be practical due to operational constraints or limitations within the process. It is crucial to take these limitations into account when making decisions regarding process optimization.

➤ *Response Table for Signal to Noise Ratios (S/N Ratios)*

Developing a Response Table for Signal to Noise Ratios (S/N ratios) in Minitab is an effective method for assessing how different factors influence performance metrics, especially within quality control, experimental design, and process enhancement. S/N ratios are crucial as they assist organizations in maximizing the "signal" (the desired output or performance) while minimizing the "noise" (unwanted variation or disturbances). This approach is extensively utilized in various industries to enhance product quality, ensure process consistency, and improve overall reliability.

To create a Response Table for S/N ratios in Minitab, the initial step involves entering experimental data into a worksheet, where the columns represent the factors being analyzed (such as type of material, temperature, or pressure) along with the associated response measurements (like yield, strength, or defect rate). After the data is organized appropriately, users can go to the "Stat" menu, select "Quality Tools," and then pick "Signal to Noise Ratios" to define the response variable and factors. Minitab then computes the S/N ratios for each factor level based on one of three response types: Larger the Better (for scenarios where higher response values are desired), Smaller the Better (for cases where lower response values are preferred), or Nominal the Best (when a specific target value is optimal). Following the S/N ratio calculations, Minitab produces a response table that shows the ratios for each factor level, enabling users to easily compare and determine which factors most significantly affect the response variable.

Table 8 Response Table for Signal to Noise Ratios

Source	DF	Adj SS	Adj MS	F-Value	P-Value
Current	2	1026.89	513.44	15.83	0.059
Voltage	2	491.56	245.78	7.58	0.117
Root Gap	2	38.22	19.11	0.59	0.629
Error	2	64.89	32.44	-	-
Total	8	1621.56	-	-	-

Residual plots serve as an essential instrument in statistical analysis for evaluating the effectiveness of a regression model. They allow us to gauge how well the model aligns with the data and detect any possible complications, such as non-linearity, inconsistent variance, or outliers. In the context of analyzing weld strength, residual plots can offer important insights into the model's sufficiency and the dependability of the forecasts. This plot assesses the normality assumption of the residuals. Ideally, the observations should align along a straight line. The points in this plot show slight deviations from a straight line, indicating some level of non-normality. Nevertheless, the deviations are not significant, suggesting that the normality assumption is reasonably upheld. This plot evaluates for non-constant variance and the presence of potential outliers.

The residuals should be randomly dispersed around zero without any identifiable pattern. This plot visually depicts the distribution of the residuals, assisting in the evaluation of the normality assumption and the detection of any outliers. The histogram displays a nearly symmetric distribution, which aligns with the normality assumption. There are no notable outliers present in the histogram. This plot examines the independence of the residuals, where the residuals should show random dispersion, lacking any recognizable pattern. The residual plots furnish crucial insights regarding the effectiveness of the regression model in estimating weld strength. Although the model seems to fit adequately, additional analysis and refinement may be required to enhance its predictive precision and stability. By addressing potential challenges and exploring alternative modeling methods, it is possible to construct more reliable and accurate models for weld strength estimation. The residuals shown in this plot are randomly scattered around zero, signifying that the model's variance is fairly steady across the fitted values range. There are no clear outliers observed in the plot.

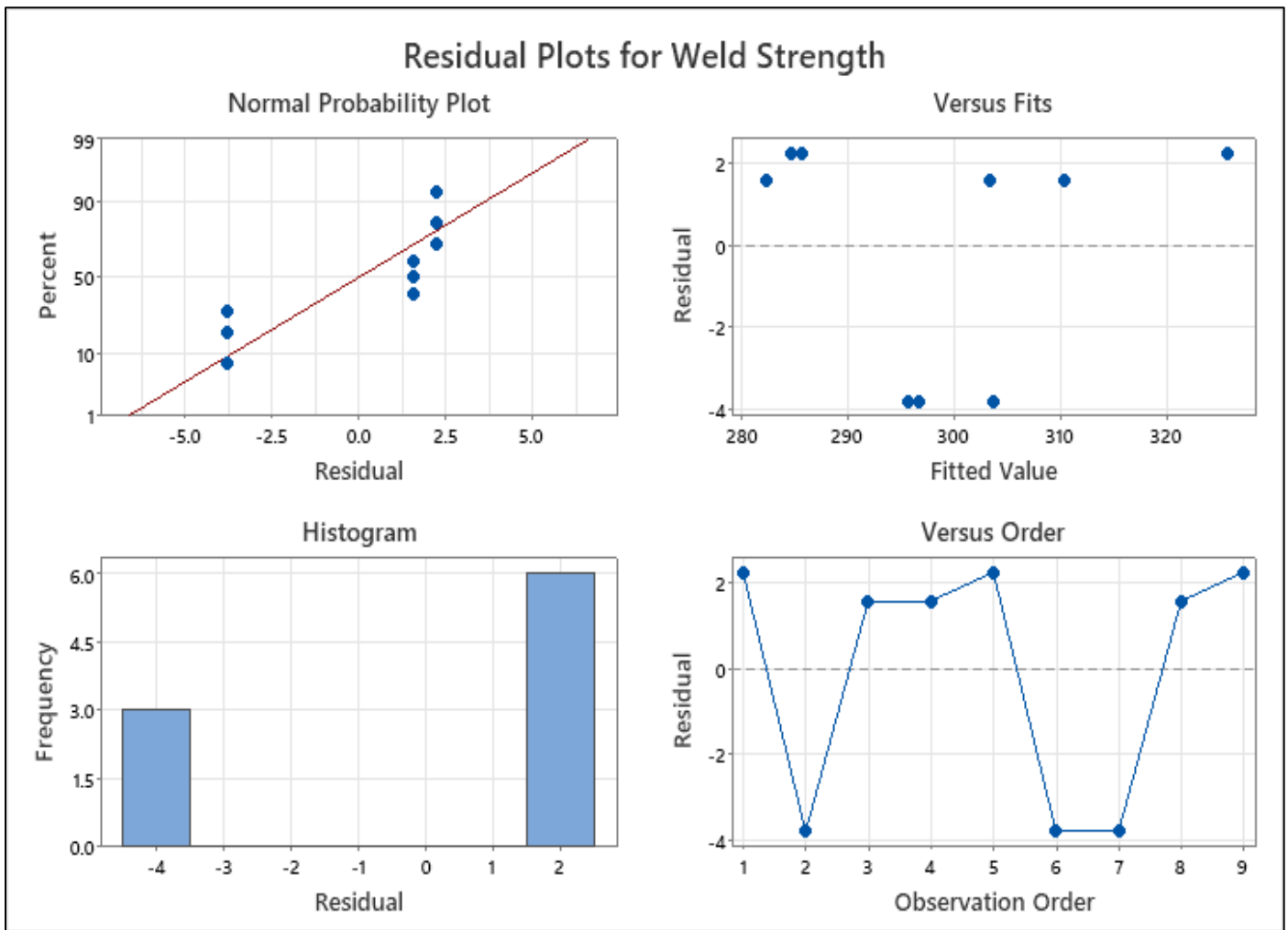


Fig 8 Residual Plots for Weld Strength

➤ *Optimization Graphs*

Creating an optimization graph in Minitab is a powerful method for visually analyzing the relationships between factors and responses, making it easier to identify the optimal conditions that enhance performance in various processes. Optimization graphs are essential tools in quality improvement projects, experimental design, and process optimization across industries such as manufacturing, pharmaceuticals, and the service sector. These graphs help organizations pinpoint the best settings for factors (independent variables) to achieve desired outcomes, ultimately improving efficiency, product quality, and customer satisfaction.

To begin creating an optimization graph in Minitab, the first step is to organize your data within a worksheet. This includes defining columns for the factors being studied (e.g., material type, temperature, speed) and the corresponding response variables (e.g., yield, strength, customer satisfaction). Organizing the data properly ensures that Minitab can accurately perform the optimization analysis. Once the data is in place, the user navigates to the "Stat" menu, selects "Quality Tools," and then chooses "Optimization." This feature enables the user to specify which response variable they want to optimize and which factors they want to analyze. Minitab allows the user to select the

type of optimization they wish to perform, such as maximizing the response (e.g., increasing product strength) or minimizing it (e.g., reducing waste or defects).

The provided plot in fig 8, a Response Surface Methodology graph, a statistical method employed to optimize processes by determining the ideal levels of input factors. In this scenario, the response variable is the Weld Strength, while the input variables are Current, Voltage, and Root Gap. The graph indicates that Weld Strength improves as one moves towards the right side. This suggests that increased levels of Current, Voltage, and Root Gap are associated with enhanced Weld Strength. The proposed optimal settings for maximizing Weld Strength are approximately Current = 120, Voltage = 24, and Root Gap = 3. Nonetheless, it is essential to mention that this is an estimation based on the plot, and additional analysis may be necessary to fine-tune the optimal settings. According to the RSM plot, it seems that elevating the levels of Current, Voltage, and Root Gap can contribute to greater Weld Strength. However, potential trade-offs and limitations related to these settings should be taken into account. Further experimentation and analysis may be required to accurately refine the optimal settings and ensure consistent achievement of the desired Weld Strength.

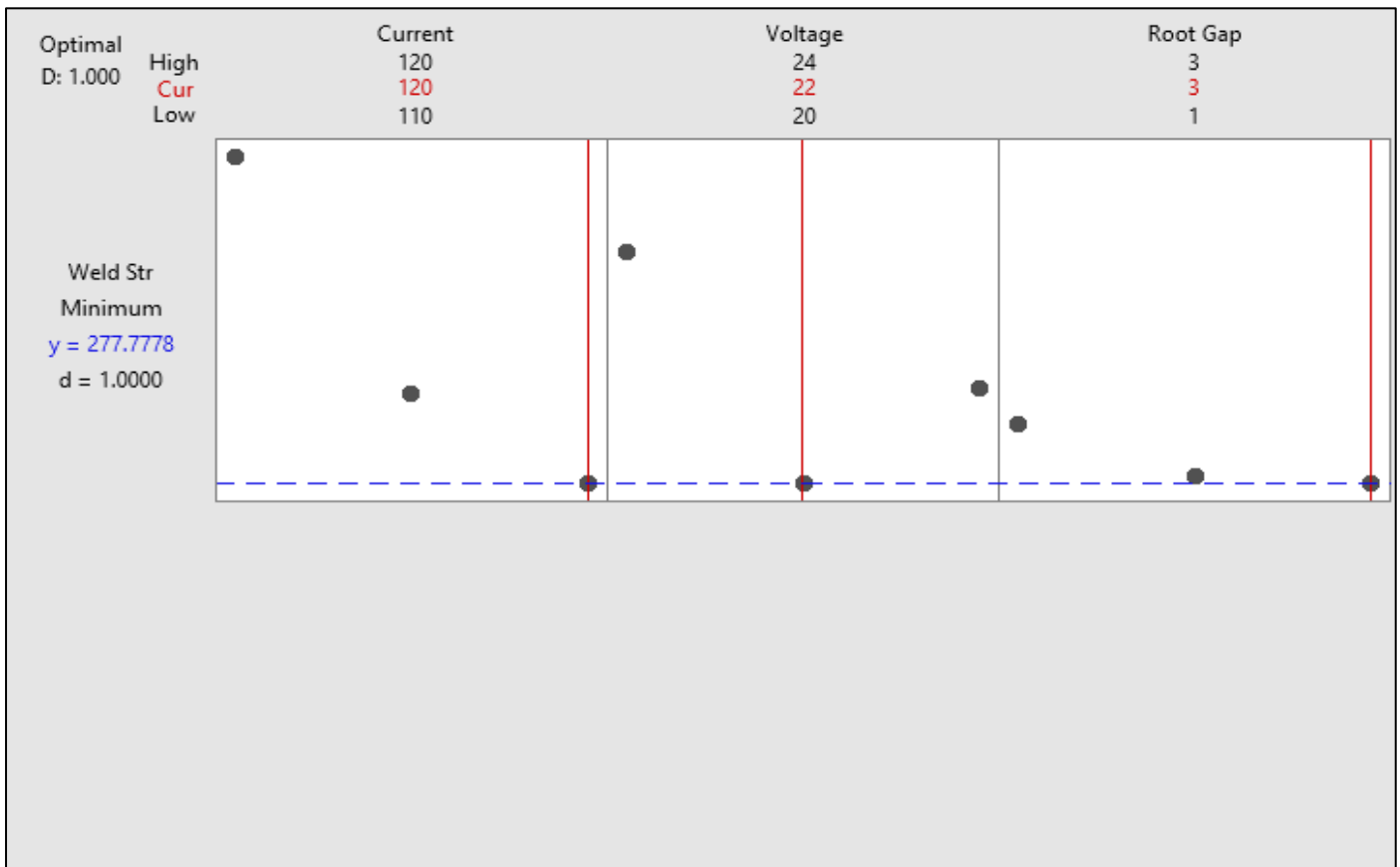


Fig 9 Optimization Graph

➤ *Interaction Plot for Weld Strength*

The interaction plot displayed illustrates how weld strength relates to three factors: Current, Voltage, and Root Gap. Each factor is assessed at three different levels, and the plot examines how strength changes across these variables and their combinations. The Current factor seems to significantly affect weld strength. As the current rises from 20 to 24, weld strength typically increases. This pattern is observed across all Voltage and Root Gap levels, indicating that higher current settings result in stronger welds. Voltage also appears to affect weld strength, but this effect is more intricate. At lower current levels (20 and 22), elevating the voltage from 20 to 24 results in a slight rise in strength. However, at the highest current level (24), increasing the voltage negatively affects strength. This interaction between Current and Voltage suggests that the ideal voltage setting varies with the current level. The Root Gap factor exhibits a distinct trend.

As the Root Gap increases from 1 to 3, weld strength steadily declines. This indicates that a smaller Root Gap is generally advantageous for achieving higher weld strength. The interaction plot offers essential insights into the connections between weld strength and the three factors. By comprehending these relationships, it becomes feasible to optimize welding parameters for desired weld strength. Additional analysis and experimentation are advised to refine the results and gain a deeper understanding of weld.

The influence of Voltage on strength varies with the Current level. When Current is low, an increase in Voltage has positive effects, whereas at higher Current levels, it can have negative effects.

The increase in strength associated with Current is more significant at smaller Root Gaps. This fig 4.3 indicates that pairing a high Current with a small Root Gap can yield exceptionally strong welds. The adverse effect of Voltage at elevated Current levels is more pronounced with larger Root Gaps. This reinforces the necessity of selecting the appropriate combination of settings. The general observation is that stronger welds are typically achieved with higher Current and smaller Root Gap. The ideal Voltage setting is contingent on the Current level. The relationship between Current and Root Gap suggests that the strongest welds can be attained by using a high Current alongside a small Root Gap. Conduct statistical analyses to assess the significance of the identified effects and interactions. Investigate the range of weld strengths achievable within the factor levels to determine the best settings for particular strength needs. Evaluate the sensitivity of weld strength to variations in factor levels to comprehend the potential effects of changes in the welding process. This indicates that pairing a high Current with a small Root Gap can yield exceptionally strong welds. The adverse effect of Voltage at elevated Current levels is more pronounced with larger Root Gaps. This reinforces the necessity of selecting the appropriate combination of settings. The general observation is that stronger welds are typically achieved with higher Current and smaller Root Gap. The ideal Voltage setting is contingent on the Current level.

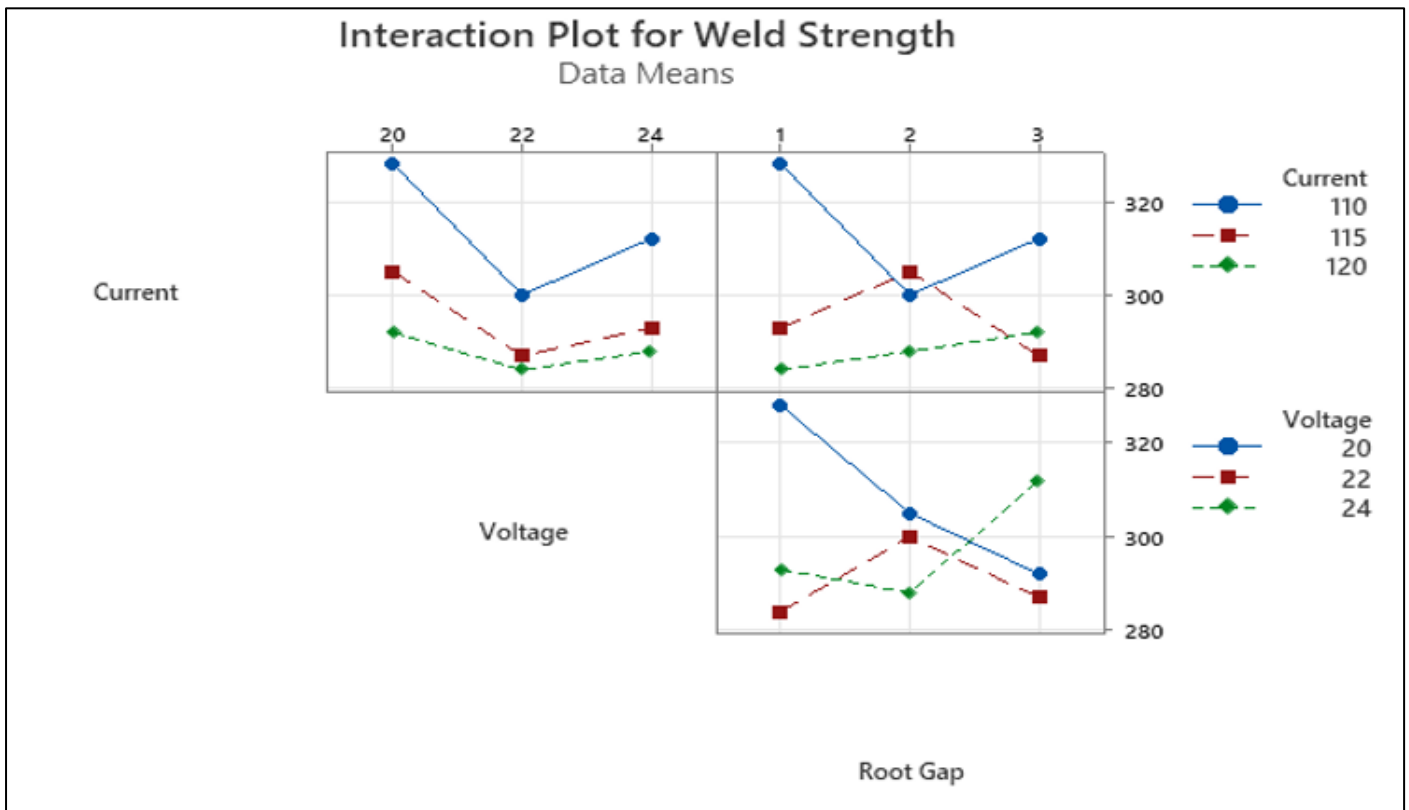


Fig 10 Interaction Plot for Weld Strength

V. CONCLUSION AND FUTURE SCOPE

This research thoroughly examined the essential factors influencing the welding strength of C45 (AISI-1045) steel through Gas Metal Arc Welding (GMAW). The investigation centered on critical variables such as arc voltage, welding current, wire feed rate, and root gap, assessing their impacts on weld quality and mechanical characteristics. Through extensive experimentation and analysis, including tensile testing and surface roughness assessment, the research pinpointed optimal parameters for enhancing weld strength. These elements have a significant effect on weld penetration, bead shape, and the heat-affected zone (HAZ). A suitable balance between arc voltage and current was discovered to yield consistent bead profiles and improved penetration, which is vital for maintaining the structural integrity of welded joints. The root gap is crucial in establishing weld fusion and preventing defects. Effective management of this factor reduces problems like incomplete fusion or excessive reinforcement, which directly affects the strength and durability of the joint. Metallurgical analyses indicated that ideal welding conditions result in refined microstructures with even grain distribution, increasing toughness and resistance to stress fractures.

Experimental findings demonstrated that welds created under optimized conditions showed higher tensile strength and hardness than those welded without optimization of parameters. This enhancement emphasizes the significance of careful selection of welding parameters. The use of advanced statistical methods, including Response Surface Methodology (RSM) and Signal-to-Noise (S/N) ratio analysis, established a strong framework for discovering and

confirming the optimal combination of parameters. The mean effect plots and optimization graphs further illustrated the interaction among different welding factors and their overall effect on weld strength.

Although this study has significantly advanced our knowledge of C45 steel's welding behavior, there are many potential research directions to explore the welding characteristics of other medium and high-carbon steels under varying GMAW conditions. Investigating these will provide a comparative insight into how different materials respond to welding parameters. It is essential to examine how various filler materials and shielding gas compositions influence weld strength and microstructure, especially in multi-material weldments. Additionally, integrating advanced welding techniques like Pulsed GMAW and Hybrid Laser-GMAW could help assess their effectiveness in enhancing weld quality and minimizing defects. For example, Pulsed welding might allow for improved control over heat input, thereby reducing HAZ distortion. Assessing the role of automation and robotics could lead to better precision and reproducibility of weld parameters, ensuring consistent weld quality in mass production settings. In-depth microstructural evaluations using methods such as Electron Backscatter Diffraction (EBSD) and Transmission Electron Microscopy (TEM) should be conducted to gain a deeper understanding of phase transformations and grain refinement processes.

Fracture mechanics investigations are warranted to analyze the performance of welded joints under various loading scenarios, including cyclic and impact loads to replicate real-world service conditions. Models should be developed to forecast thermal distribution and residual

stresses throughout the welding process, as understanding and addressing residual stresses could boost fatigue life and diminish the risk of stress-induced failures. Furthermore, examining post-weld heat treatments (PWHT) could reveal their effectiveness in alleviating residual stresses and enhancing weld toughness. It is also vital to assess the ecological effects of different welding processes and materials. Future research could concentrate on cultivating sustainable welding practices that minimize emissions and energy usage. Conducting cost-benefit assessments may provide insights into the economic viability of adopting optimized welding parameters in industrial contexts, facilitating the implementation of best practices without compromising financial performance. Expanding mechanical testing to encompass fatigue, corrosion resistance, and creep evaluations will offer a thorough assessment of welded joints' durability over time.

Collaborating with standardization organizations to revise welding codes and guidelines based on recent research findings is essential for ensuring widespread industry adoption of optimal practices. The potential application of optimized welding techniques in emerging fields such as renewable energy sources (like wind turbines), electric vehicles, and aerospace should also be explored. These sectors necessitate high-strength, lightweight materials that can take advantage of advanced welding innovations. Additionally, examining the conjunction of additive manufacturing (3D printing) with conventional welding methods for developing complex structures with superior mechanical characteristics is valuable. This research highlights the critical role of optimizing parameters to enhance the strength and quality of welds in C45 steel. By methodically investigating the influences of arc voltage, welding current, and root gap, this study establishes a solid groundwork for future developments in welding technology. Ongoing inquiry into advanced methods, materials, and predictive models will not only advance the field of welding engineering but will also facilitate the creation of stronger, more dependable structures across various sectors. The findings derived from this study lay the groundwork for innovations that hold the potential to revolutionize manufacturing processes, enhance product lifespan, and contribute to the continued evolution of industrial welding standards.

REFERENCES

- [1]. SANJAY KUMAR GUPTA, SHIVANSH MEHROTRA, AVINASH RAVI RAJA, M. VASHISTA AND M.Z. KHAN YUSUFZAI, Effect of Welding Speed on Weld Bead Geometry and Percentage Dilution in Gas Metal Arc Welding of SS409L, ICMPC-2019
- [2]. MARTINEZ, ROGFEL THOMPSON, GUILLERMO ALVAREZ BESTARD, SADEK C. ABSI ALFARO. Two gas metal arc welding process dataset of arc parameters and input parameters. Data in Brief, 35 (2021), pp. 106790.
- [3]. G. CHAUDHARI, PAVAN, PRIYANK B. PATEL, JAKSAN D. PATEL. Evaluation of MIG welding process parameter using Activated Flux on SS316L by AHP-MOORA method. Materials today: proceedings, 5.2 (2018), pp. 5208-5220.
- [4]. LERMEN, RICHARD THOMAS, ANDERSON DAL MOLIN, DJEISON RANGEL BERGER, VALTAIR DE JESUS ALVES, CAMILA PEREIRA LISBOA. Optimization of parameters on robotized gas metal arc welding of LNE 700 high-strength steel. Journal of Manufacturing and Materials Processing, 2-4 (2018), pp. 70.
- [5]. TAGIMALEK, HADI, MAJID AZARGOMAN, MOHAMMAD REZA MARAKI, MASOUD MAHMOODI. The effects of diffusion depth and heat-affected zone in NE-GMAW process on SUH 310S steel using an Image processing method. International Journal of Iron and Steel Society of Iran, 17- 1 (2021): 11-20.
- [6]. PARK, JIN-HYEONG, SUNG-HWAN KIM, HYEONG-SOON MOON, MYUNGHYUN KIM, and DAE-WON CHO. Effect of process parameters on root pass welding and analysis of microstructure in V-groove pulsed gas metal arc welding for mild steel. The International Journal of Advanced Manufacturing Technology, 109-7 (2020).
- [7]. HACKENHAAR, WILLIAM, ARNALDO R. GONZALEZ, IVAN G. MACHADO, JOSÉ AE MAZZAFERRO. Welding parameters effect in GMAW fusion efficiency evaluation. The International Journal of Advanced Manufacturing Technology, 94-1 (2018).
- [8]. WINCZEK, JERZY, MAREK GUCWA, MILOŠ MIČIAN, AND KRZYSZTOF MAKLES. Numerical analysis of the influence of electrode inclination on temperature distribution during GMAW overlaying. Mathematical Problems in Engineering, 2019 (2019).
- [9]. DAGOSTINI, VINICIUS DOS SANTOS, ARIANE NEVES DE MOURA, TEMÍSTOCLES DE SOUSA LUZ, NICOLAU APOENA CASTRO, MARCOS TADEU D'AZEREDO ORLANDO, ESTÉFANO APARECIDO VIEIRA. Microstructural analysis and mechanical behaviour of the HAZ in an API 5L X70 steel welded by GMAW process. Welding in the World, 65-6 (2021).
- [10]. SINGH, VIVEK, M. CHANDRASEKARAN, SUTANU SAMANTA. Study on the influence of heat input on mechanical property and microstructure of weld in GMAW of AISI 201LN stainless steel. Advances in Materials and Processing Technologies, (2020), pp. 1-11.
- [11]. CHO, DAE-WON, JIN-HYEONG PARK, AND HYEONG-SOON MOON. A study on molten pool behaviour in the one pulse one drop GMAW process using computational fluid dynamics. International Journal of Heat and Mass Transfer, 139 (2019), pp.848-859.

- [12]. LEE, HUIJUN, CHANGWOOK JI, JIYOUNG YU. Effects of welding current and torch position parameters on bead geometry in cold metal transfer welding. *Journal of Mechanical Science and Technology*, 32.9 (2018), pp. 4335- 4343.
- [13]. SAHA, MANAS KUMAR, RITESH HAZRA, AJIT MONDAL, SANTANU DAS. Effect of heat input on geometry of austenitic stainless steel weld bead on low carbon steel. *Journal of the Institution of Engineers (India): Series C*, 100-4 (2019), pp. 607-615.
- [14]. ALBANNAI, A., ALORAHER, A., ALASKARI, A., ALAWADHI, M., & JOSHI, S. Effects of tandem side-by-side GTAW welds on centreline solidification cracking of AA2024. *Manuf Technol*, 21, (2021). 150-162.
- [15]. SEJČ, P., & BELANOVÁ, J. The effect of welding parameters on the properties of joint between studs and steel sheet USIBOR Type 22MnB5. *Manuf Technol*, 19(3), (2019), 492-498.
- [16]. BRABEC, J., JEŽEK, Š., BENEŠ, L., KŘÍŽ, A., & MAJRICH, P. Suitability confirmation for welding ultra-high strength steel S1100QL using the Rapid Weld method. *Manuf Technol*, 21(1), (2021), 29-36.
- [17]. VIJAYAKUMAR, A. PRADEEP, PALANIVEL SATISHKUMAR, BHARAT SINGH, VIJAY KUMAR SHARMA, Optimization of process variables for shielded metal arc welding dissimilar mild steel and medium carbon steel joints, 24 Jun 2023 - pp 1-18.
- [18]. MEHMET ŞÜKRÜ ADIN, BAHATTIN İŞCAN20, Optimization of process parameters of medium carbon steel joints joined by MIG welding using Taguchi method, Mar 2022 - European mechanical science- Vol. 6, Iss: 1, pp 17-26.
- [19]. S. S. AMARAPURE, RATAN A. PATIL, Experimental Investigation of TIG Welding Parameters and Weld Joint Strength for Carbon Steel - SA516GR70 Material based on Taguchi Method, 08 Mar 2022 - Vol. 14, Iss: 2
- [20]. DESHMUKH, YOGESH SHIRISH MANOJ, Investigation of Process Parameters on Strength of Welding Joint in GMAW, 22 Mar 2022 - pp 568-574.